Ti leaching from activated ilmenite–Fe mixture at different milling energy levels

Elham Hosseini, Fereshteh Rashchi, and Abolghasem Ataie

School of Metallurgy and Materials Engineering, College of Engineering, University of Tehran, P.O. Box 11155/4563, Tehran, Iran
(Received: 14 January 2018; revised: 11 May 2018; accepted: 23 May 2018)

Abstract: Mechanical activation processes on ilmenite concentrate were performed in three different energy levels. Iron powder as a reducing agent was added to ilmenite in the milling stage and the mechanically activated mixture was subjected to acid leaching. The leaching experiments were designed using the Taguchi method, and the optimum ranges were obtained. Furthermore, response surface methodology (RSM) was used to optimize the critical parameters in the leaching system to achieve the highest titanium (Ti) leachability. Based on the inductively coupled plasma-optical emission spectrometry (ICP-OES) results, maximum leaching recovery of Ti (80%) was obtained using activated Ti concentrates at a medium activation energy level, which is calculated to be 25.38 kJ/g, using 15vol% hydrochloric acid (HCl), a temperature of 70°C, leaching time of 3 h, and a solid-to-liquid ratio of 0.05 g·mL^{-1}. Intensifying the milling energy from a low to high level led to a decrease in the mean crystallite size and also structure homogenization at the high energy level. According to the transmission electron microscopy (TEM) images, the mean grain size of the ilmenite/Fe nanocomposite was about 30 nm at the medium energy level sample. Finally, solvent extraction by tributyl phosphate (TBP) was performed on the leach liquor to separate dissolved Fe (the major impurity) from Ti, which led to 83% extraction recovery of Ti.

Keywords: ilmenite; leaching; titanium extraction; mechanical activation

1. Introduction

Titanium dioxide (TiO$_2$) is a white opaque material, highly resistant to color change and suitable for coatings. Therefore, TiO$_2$ pigments have been used in a wide range of applications in various industries such as paint, paper, fibers, cosmetics, food, and optical coatings, including dispersion of radiation and antireflection coatings and humidity sensors [1].

Titanium dioxide is commercially manufactured via the following two main processes: (1) "sulfate process" and (2) "dry chlorination" [2–5]. Sulfate process is a relatively durable method that requires a high consumption of sulfuric acid, which can ultimately lead to water contamination [6–7]. Today, about 60% of the total TiO$_2$ in the world is produced via chloride method [8]. The raw material used in this method is natural or synthetic rutile. Lack of natural Ti resources, and in particular rutile, has steered researchers toward the manufacture of synthetic rutile from ilmenite ore for use in chloride process [8]. Production of synthetic rutile from ilmenite is possible via hydrometallurgy and pyrometallurgy routes.

In recent years, researchers have developed the use of direct hydrometallurgical procedures using acidic media to produce synthetic rutile as it is significantly environment friendly in many aspects. Table 1 illustrates some of the recent work on ilmenite leaching to produce rutile. In some of these studies, iron powder has been added as a reducing agent in the leaching stage using an autoclave at temperatures above 100°C to reach high leaching recovery of Ti [9–10]. Additionally, some of the studies utilize pressure leaching of ilmenite or leaching at very high temperatures followed by various processes to obtain high purity TiO$_2$ crystalline structures [11]. In all of the mentioned studies, high temperatures and extended time periods were employed, minimizing the applicability at large scales.

🖄 Springer

Table 1.   Summary of previous work on ilmenite leaching to produce rutile

Method	Pre-treatment of ilmenite/additives	Optimum leaching conditions	Reference No.
Sulfuric acid leaching	Mechanical activation by milling	H_2SO_4, 15vol%; temperature, 100°C; time, 4 h	[7]
Reductive leaching with hydrochloric acid	Fe as reducing agent added to the leaching solution	HCl, 20vol%; temperature, 110°C; time, 5 h	[9]
Reductive leaching with hydrochloric acid	Fe as reducing agent added to the leaching solution	HCl, 20vol%; temperature, 110°C; time, 6 h	[10]
Pressure leaching with hydrochloric acid	No pre-treatment/no additive	HCl, 20vol%; temperature, 140°C; time, 4 h	[11]
Hydrolysis of $TiOCl_2$ obtained from low grade ilmenite leach liquor	No pre-treatment/no additive	HCl, 20vol%; temperature, 70°C; time: 3 h	[12]

The speciation of Ti in hydrochloric acid solutions significantly affects its extraction behavior while using various extractants. The Ti species present in acidic media remains controversial [13]. For example, whether the divalent titanyl ion exists as TiO^{2+} or $[Ti(OH)_2]^{2+}$ [14] has resulted in different interpretations of Ti(IV) extraction mechanisms for similar extraction systems. According to the Pourbaix diagram of the titanium–water system reproduced by Sole [15], acid activity of greater than 1 M yields TiO^{2+} as the dominant species in the aqueous solution, whereas solutions with a pH value greater than 5 allows Ti(IV) to form $TiO_2 \cdot H_2O$ precipitate. In chloride solutions, TiO^{2+} tends to combine with Cl^- to form different complexes. At chloride ion concentrations of about 4.5 M, the neutrally charged $TiOCl_2$ has been suggested to be the dominant species [16].

To the best of our knowledge, few studies have been conducted in ilmenite leaching system at atmospheric pressure and low temperatures [12]. In the present study, the effect of adding iron powder to the ilmenite concentrate in the milling stage (instead of the leaching solution) was investigated. It was assumed that there are different mechanisms activating the mineral structure, such as dissolving the iron in ilmenite structure, and formation of crystal defects (such as dislocations, vacancies, stacking faults, and grain boundaries). The generation of high defect densities enhances the diffusivity of the reactants and increases the number of nucleation sites. Furthermore, the microstructural refinement induced by mechanical activation decreases the diffusion distances [17].

The main intention of the current study is to enhance the leaching efficiency of Ti from ilmenite concentrates at "lower temperatures" and "shorter time intervals" than those reported in previous reports. In this regard, effects of mechanical activation and use of iron powder in the milling stage on the leaching of ilmenite concentrates have been investigated. Additionally, influences of the process parameters such as milling energy and leaching conditions are discussed. Finally, separation/purification of Ti from Fe (considered as the major impurity in the leaching solution) in solution is studied using solvent extraction with tributyl phosphate (TBP) in kerosene as the extractant.

2. Theory

The milling process of the initiators (ilmenite + Fe) is influenced by milling parameters such as ball-to-powder mass ratio (BPR), rotation speed, size of the balls, and milling time. All the results and the activation mechanism can be discussed and analyzed if the milling parameters are stated as a single term, "milling energy". Thus, in this study, the total produced energy via ball milling was calculated for three different energy levels. The energy released by each ball per hit during the milling process is given by the following equation [18–20]:

$$\Delta E_b = \frac{1}{2} m_b (V_b^2 - V_s^2) \tag{1}$$

where m_b is the ball mass, and V_b and V_s are the absolute velocity before and after the hit, respectively. ΔE_b can be calculated based on the method suggested by Burgio *et al.* as defined by the following [18]:

$$\Delta E_b = -m_b[\omega_v^3(R_v - r_b)/\omega_p + \omega_p\omega_v R_p](R_v - r_b) \tag{2}$$

where ω_p and ω_v are the absolute angular velocity of the mill plate and of one vial, respectively. R_p, R_v, and r_b are the radii of plate, vial, and ball, respectively. The energy released by one ball in a vial containing N_b balls can be obtained as $\Delta E_b^* = \varphi_b \Delta E_b$ where $\varphi_b < 1$ is an empirical factor for various levels of filling of the vial. Finally, the total energy transferred per unit mass of powder for a given milling time, t, can be written as follows:

$$\Delta E_t = \frac{\Delta E_b^* N_b f_b t}{W_P} \tag{3}$$

where W_p is the powder mass in the vial and f_b is the frequency with which the balls are launched and can be stated as follows:

$$f_b = K \frac{(\omega_p - \omega_v)}{2\pi} \tag{4}$$

where K is the proportionality constant, and it equals about 1.

The above parameters were calculated for three different milling energy levels evaluated in this study and are presented in Table 2.

Table 2. Milling conditions, milling energy parameters, and energy levels of the samples (ball diameter of 15 mm)

Energy level	Rotation speed / (r·min⁻¹)	Milling time / h	Ball-to-powder mass ratio (BPR)	φ_b	ΔE_b / J	f_b / s⁻¹	ΔE_t / (kJ·g⁻¹)
Low	200	2	10	0.99	0.02895	7.5	2.590
Medium	250	5	20	0.95	0.07654	12.5	25.379
High	300	10	30	0.89	0.10417	15.0	132.633

3. Experimental

3.1. Materials and analysis

All the chemical reagents used in this study were of analytical grade. Deionized water was used throughout the experiments. Ilmenite concentrate (from Kahnuj, Iran) with an average particle size of 200 μm (analyzed by laser particle size analysis (LPSA, CILAS 1064)) was used as a source of Ti. Iron powder (99.9%) was utilized as a reducing agent. The organic solvent used in this work was industrial-grade TBP from Merck, Germany. The extractants were used without further purification. Kerosene from Tehran Oil Re-

finery Co., Iran was used as a diluent. Hydrochloric acid (HCl, 37% pure) and $CaCl_2 \cdot 2H_2O$ (99.9%) from Merck, Germany, were used as the leaching agent and the $[Cl^-]$ modifier, respectively. Chemical composition of the ilmenite concentrate was analyzed by X-ray fluorescence (XRF) (Philips/PW1480) and is shown in Table 3. This analysis shows that TiO_2 and Fe_2O_3 are the main oxide compounds detected in the ilmenite used in the present study. Fig. 1 depicts the X-ray diffraction (XRD) pattern of the concentrate. It is evident from Fig. 1 that $FeTiO_3$ is the main phase of the concentrate and Fe_2O_3 is the second major phase.

Table 3. Chemical composition of the ilmenite sample by XRF wt%

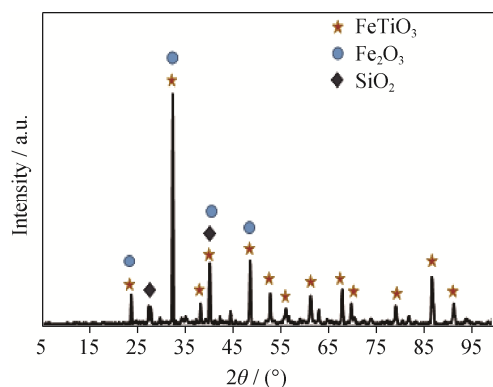| Al_2O_3	P_2O_5	CaO	SiO_2	TiO_2	Fe_2O_3	S	MgO	K_2O	MnO
0.890	0.116	1.840	4.560	46.890	43.680	0.015	0.950	0.010	0.963

Fig. 1. XRD pattern of ilmenite concentrate.

3.2. Mechanical activation process

A mechanical activation process was performed using a planetary ball mill at room temperature and atmospheric pressure. Mechanically activated ilmenite concentrate was prepared as follows: 7.2 g ilmenite concentrate and a stoichiometric amount of iron powder (3.8 g) as the reducing

agent [9] were mixed together, and each milling vial was charged with this powder mixture. Starting materials contained no moisture. To activate the concentrate, three energy levels (herein labeled as low, medium, and high) were applied to the mixtures. Milling conditions at each level are shown in Table 2. To study the phase changes resulting from the milling process, XRD was performed using a Philips-3040/60 PW diffractometer (Cu K$_\alpha$), and the patterns obtained were analyzed using X'Pert High Score Plus software. Energy dispersive X-ray spectroscopy (EDS) point analysis of the activated samples was conducted by Bruker Co. MV2300 model. High resolution scanning electron microscopy (HRSEM) and transmission electron microscopy (TEM) images were taken by Cam Scan and Philips CMC model, respectively.

3.3. Leaching process

A 500 mL three-necked glass reactor equipped with a refluxing condenser with a magnetic stirring bar (length of

20 mm) was filled with preheated HCl solution. A thermometer was placed in one neck to control the temperature variation. The other neck was used for pH control or to add ingredients. The reactor was placed in a sand bath and the whole set-up was placed on a magnetic stirrer equipped with a heating system. Good mixing was consistently obtained to prevent deposition in the solution. Upon completion of the leaching, the solution was filtered, and the residue was isolated. To measure the solubility of Ti in the leaching solution, an inductively coupled plasma-optical emission spectrometry (ICP-OES) Varian VISTA-PRP model was employed.

(1) Un-milled ilmenite.

In the leaching experiment, 200 mL of HCl solution (20vol%) was heated to 90°C. The experiment commenced with the addition of 10 g un-milled ilmenite followed by the addition of a stoichiometric amount of iron powder after 20 min. The leaching experiments were performed for 6 h [10].

(2) Milled/Activated ilmenite.

After reaching the desired temperature, 10 g of the activated ilmenite was allowed to leach based on the time periods established in the designed experiments (Tables 4 and 5).

3.4. Design of experiments (DOE)

To minimize the number of experiments and optimize the parameters involved in the processes, experimental design was applied using the Taguchi method and response surface methodology (RSM). In the first step, the Taguchi method was used for screening tests [21–22]. This method uses a limited number of experiments and different variables can be examined concurrently [21,23]. Table 4 tabulates the design of experiments using the Taguchi method and the associated responses. In the next step, RSM was used to optimize the ranges of effective parameters and their levels (see Table 5). The purpose of this step was to generate a model that could estimate maximum Ti recovery. Titanium recovery is a term indicative of dissolved Ti in leach liquor and can be calculated as follows:

$$\text{Ti recovery} = \frac{\text{Ti}_d}{\text{Ti}_t} \times 100\% \tag{5}$$

where, Ti_d and Ti_t are the mass of dissolved titanium and the mass of total titanium in ilmenite, respectively. Design and statistical analysis of experiments was done by Design-Expert 7 (State-Ease, Inc.) software. The experiments were performed in a random order to ensure that the uncontrolled parameters had the least effect on the results [22]. To improve the precision of the model, six center points were employed.

Table 4.   Ti leaching parameters (Taguchi method)

Run	Temperature / °C	Time / h	Solid-to-liquid ratio / $(g·mL^{-1})$	HCl concentration / vol%	Milling energy	Ti Recovery / %	HCl concentration / $(mol·L^{-1})$
1	70	3.0	0.10	15	Medium	62	1.32
2	90	4.5	0.10	10	Low	7	0.88
3	90	6.0	0.07	5	Medium	0	0.63
4	70	3.0	0.05	5	Low	7	0.88
5	80	3.0	0.07	15	Low	28	1.89
6	70	6.0	0.10	5	Low	4	0.44
7	70	4.5	0.05	5	High	25	0.88
8	90	4.5	0.05	15	Low	35	2.65
9	90	3.0	0.10	10	High	39	0.88
10	80	4.5	0.10	5	Medium	41	0.44
11	90	3.0	0.07	5	High	0	0.63
12	70	6.0	0.07	10	Low	13	1.26
13	80	3.0	0.05	10	Medium	58	1.76
14	80	4.5	0.07	15	High	70	1.89
15	70	6.0	0.10	15	High	66	1.32
16	70	4.5	0.07	10	Medium	47	1.26
17	80	6.0	0.05	10	High	75	1.76
18	90	6.0	0.05	15	Medium	82	2.65

Table 5. Ti leaching parameters (RSM)

Run	Temperature / °C	Solid-to-liquid ratio / $(g \cdot mL^{-1})$	HCl concentration / vol%	Ti Recovery / %	HCl concentration / $(mol \cdot L^{-1})$
1	70	0.10	15.0	77	1.32
2	75	0.08	12.5	52	1.37
3	80	0.10	10.0	51	0.88
4	75	0.08	16.7	76	1.84
5	70	0.05	15.0	80	2.65
6	75	0.08	12.5	65	1.37
7	80	0.10	15.0	70	1.32
8	75	0.08	8.3	46	0.91
9	80	0.05	15.0	75	2.65
10	70	0.05	10.0	62	1.76
11	75	0.08	12.5	67	1.37
12	75	0.03	12.5	80	3.68
13	75	0.12	12.5	44	0.92
14	80	0.05	10.0	68	1.76
15	75	0.08	12.5	68	1.37
16	90	0.10	10.0	51	0.88
17	75	0.08	12.5	69	1.37
18	75	0.08	12.5	66	1.37

3.5. Solvent extraction process

In the optimum leaching condition, 10 g ilmenite ore was dissolved in 2.65 M HCl (100 mL) at 70°C. The titration and ICP-OES analyses revealed that the solution contained 25.87 g/L of Fe and 9.86 g/L of Ti, respectively. Other metal ions including Ag, Ca, Mn, Pb, Mg, and Sn species were also present in trace concentrations (< 2 mg/L). To separate Ti from Fe rich leach liquor, solvent extraction experiments were conducted using 1.82 M of TBP diluted in kerosene (25 mL TBP in 25 mL kerosene). The organic phase composition contained 50vol% of the extractant (TBP) and 50vol% kerosene. The extraction process was implemented at (25 ± 2)°C and an organic to aqueous phase volume ratio (O/A) of 1:1. The aqueous and organic phases were stirred by a magnetic stirrer for 30 min in three different [Cl⁻] concentrations of 2.65 M (initial concentration), 6 M, and 10 M. The additional [Cl⁻] was adjusted using $CaCl_2 \cdot 2H_2O$. After stirring, phase separation of the solution mixture was performed by allowing the solution to settle. The concentration of the Ti left in the aqueous phase was analyzed using ICP-OES. To determine the Fe concentration and speciation in the solution, the total amount of Fe was first analyzed via ICP-OES method followed by a titration method, which found the amount of Fe^{3+} to be negligible. Therefore, it was concluded that the total Fe was in the form of Fe^{2+} (which could not be extracted by TBP), and its concentration was analyzed via

the redox titration method [24].

4. Results and discussion

4.1. Mechanical activation

To determine the effect of adding Fe powder as a reducing agent in the milling stage, ilmenite concentrate was activated in three energy levels (Table 2) without the addition of Fe. It can be observed from the related XRD patterns (Fig. 2) that, regardless of milling energy, $FeTiO_3$ is the only detectable
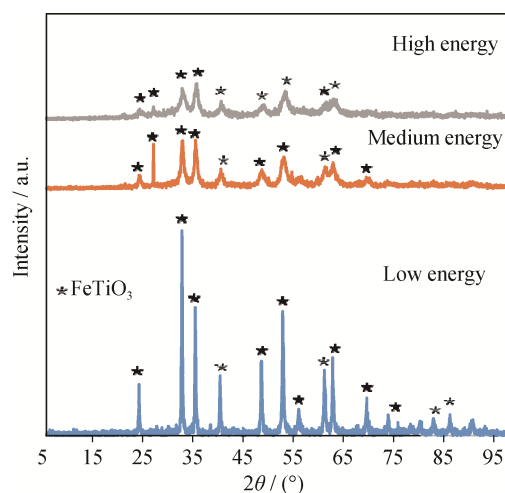

Fig. 2. XRD patterns of the samples milled under various milling energies (without Fe addition).

phase. Additionally, SiO_2 and Fe_2O_3 peaks (shown up in Fig. 1) disappear in all three patterns, which may be because of amorphization or grain refinement. Significant peak broadening during energy increment in the activation process was mainly due to the ilmenite crystallite refinement and its amorphization.

Fig. 3 illustrates the XRD patterns of the samples listed in Table 2. According to the low energy XRD pattern, it is evident that the insufficient energy at this level enables the crystalline structure of the ilmenite ($FeTiO_3$) to remain unaffected and the concentrate's main peaks are clearly distinguishable. The peaks are sharp, showing the relatively coarse crystallite size of ilmenite. As expected, intensifying the milling energy from a low to high level led to the broadening of peaks in the XRD pattern, indicative of a decrease in crystallite sizes and the formation of partially amorphous structures. In the low energy sample, ilmenite is the dominant phase; however, Fe peaks are also observed. Increasing the milling energy to medium shows a noticeable decrease in the intensities of the ilmenite peaks and the appearance of Fe_2O_3 peaks in the XRD pattern. Partial oxidation of Fe particles during the milling process or a reduction reaction of ilmenite with Fe could be responsible for the existence of the Fe_2O_3 phase. The absence of the reduction peaks of the reaction product could be attributed to its low amount and the formation of amorphous structures. As the milling energy increases to reach the highest level, the corresponding ilmenite peaks are broadened and their intensities are reduced, thus indicating

of the crystallite size decreasing. Regarding the XRD patterns, no new composition is formed; thus, it can be assumed that the brittle crystalline $FeTiO_3$ particles are fully embedded in ductile Fe particles as a parent phase.
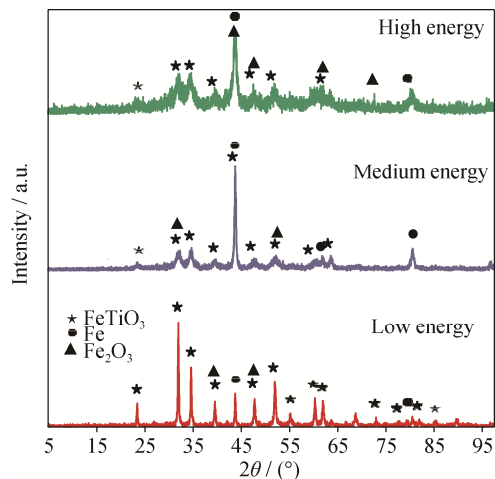

Fig. 3. XRD patterns of the samples milled in the presence of iron powder under various milling energies.

The EDS maps of the mechanically activated milled mixtures at low and medium energy levels are shown in Fig. 4. According to Fig. 4, the energy increment of the powder (mixture of ilmenite and Fe) from the low to medium resulted in structure homogenization. The obtained mass distribution from the medium energy sample from EDS point analysis shown in Fig. 5 confirmed the XRF results of the ilmenite concentrate.
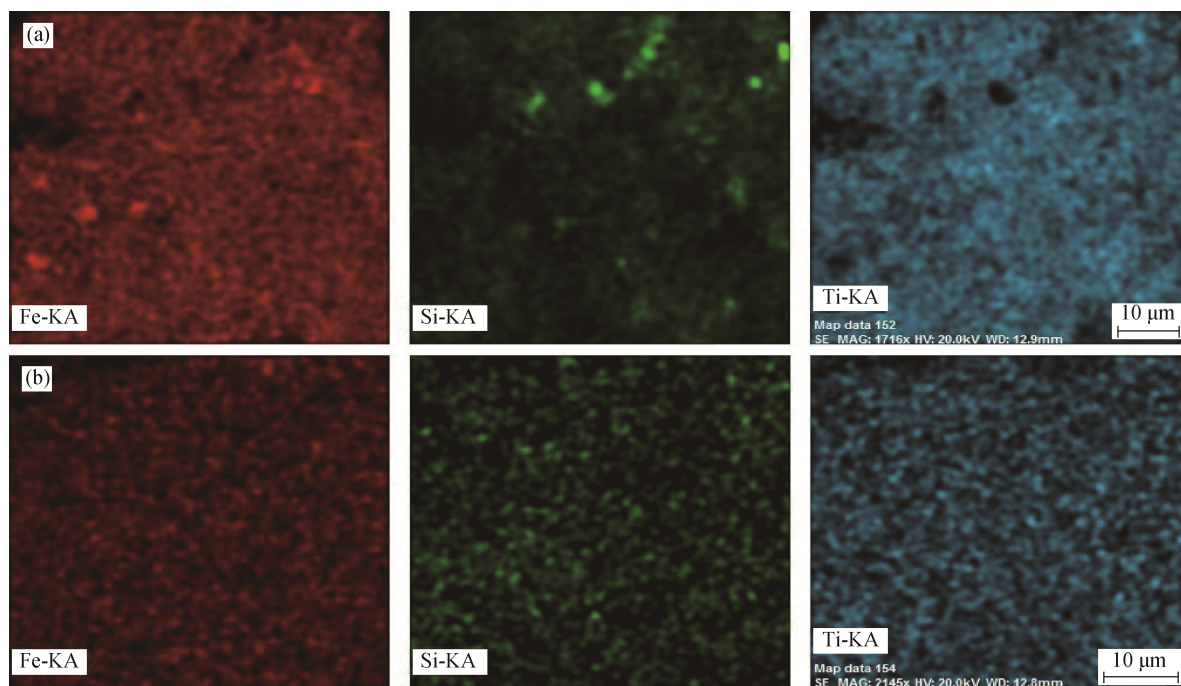

Fig. 4.   EDS maps of main elements (Fe, Si and Ti) of ilmenite composition for different ball milling energies: (a) low energy; (b) medium energy.
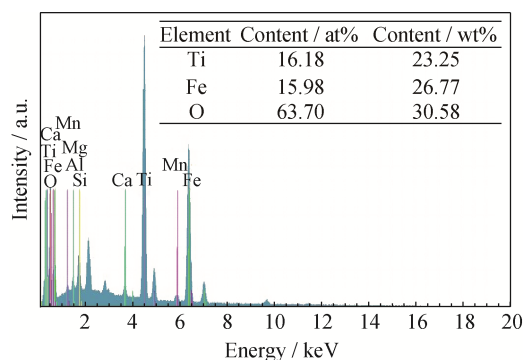
Element	Content / at%	Content / wt%
Ti	16.18	23.25
Fe	15.98	26.77
O	63.70	30.58

Fig. 5.   EDS point analysis of medium energy milled sample.

Figs. 6(a)–6(c) shows the HRSEM images of low, medium, and high energy mechanically activated samples. These figures depict the effect of milling energy on the morphology and crystallite size of the products considering agglomeration. The particles were subjected to cold welding and fracturing that occurred repeatedly during the milling process. Agglomerated particles could be observed in all three samples (figures not shown here). The edges of the particles seen in Fig. 6(a) are the sharpest, thus indicating that increasing the milling energy tends to round off the sharp edges of the particles, as shown in Fig. 6(c).

Fig. 6.   HRSEM micrographs of milled sample after mechanical activation at (a) low, (b) medium, and (c) high activation energies.

Fig. 7 shows the TEM images of the activated ilmenite concentrate at the medium energy level, which was the most homogenized and fine-grained sample. The particles have almost irregular shapes and the contrast shown in different parts within particles confirms the nanocomposite nature of the sample. The particles comprise nanometer-sized crystallites ranging from 20 to 300 nm with a mean particle size of 30 nm, suitable for rapid leaching. The presence of large particles indicates the occurrence of the microwelding and subsequent agglomeration.

4.2. Leaching

To observe the effect of mechanical activation on the leaching performance, Ti leaching recovery of the un-milled ilmenite in the presence of Fe (performed under vigorous conditions: HCl concentration of 20vol%, leaching temperature of 90°C, and leaching time of 6 h) was compared with the activated mixture of ilmenite and Fe. Despite the presence of Fe as a potential reducing agent, the results from ICP-OES analysis for the un-milled sample showed that recovery of Ti in the obtained leach liquor was less than 10%. However, using the milled mixture, up to 80% Ti was recovered. The significant effect of mechanical activation on the improved Ti recovery is due to the application of mechanical activation as an innovative procedure, which leads to reactivity and enhanced leaching ability of the concentrate obtained via a combination of a new surface area, an increase in internal and surface energy, and the formation of crystalline disorder in mineral.
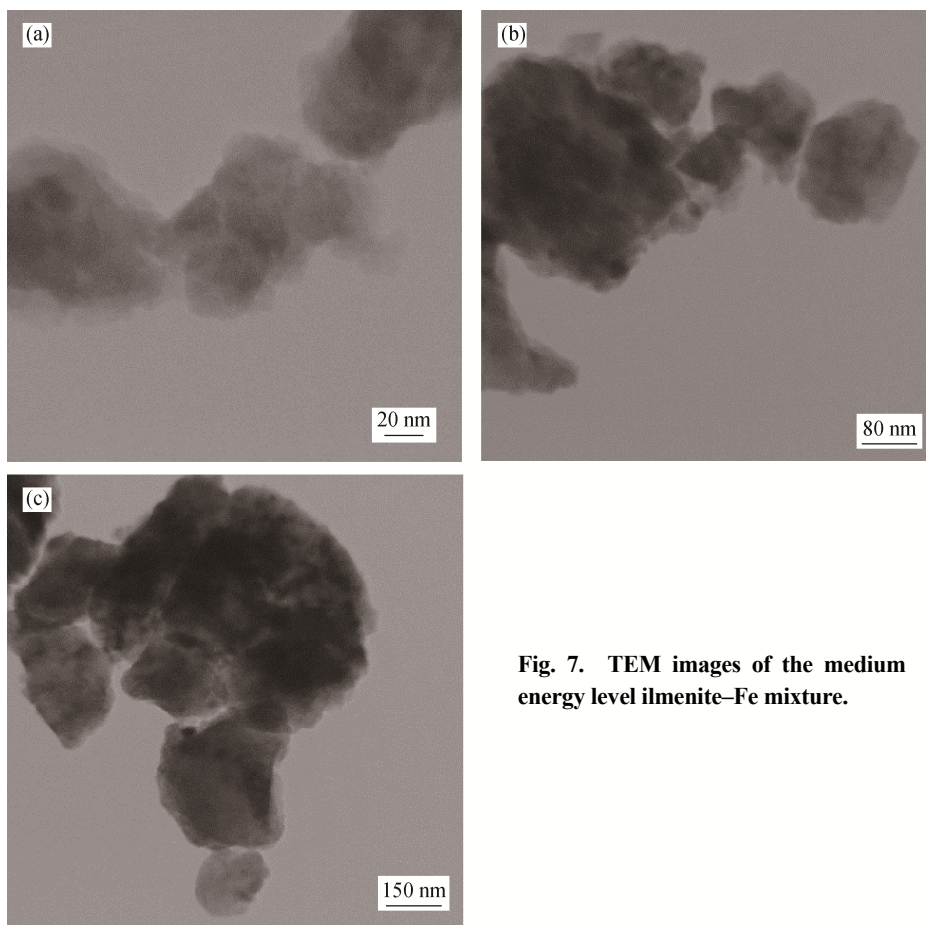
1270

Int. J. Miner. Metall. Mater., Vol. 25, No. 11, Nov. 2018

Fig. 7. TEM images of the medium energy level ilmenite–Fe mixture.

Fig. 8 shows the effect of temperature, time, sol-id-to-liquid (S/L) ratio, HCl concentration, and milling energy on ilmenite leaching. According to Fig. 8(a), as the temperature increases from 70 to 80°C, Ti recovery enhances, and it decreases with further temperature increment. Fig. 8(b) shows that increasing the leaching time caused no significant increase in Ti recovery. Thus, it seems that the leaching time was not an effective parameter in the selected range. Therefore, 3 h of leaching was considered to be the optimum time for the experiment. According to Fig. 8(c), increasing the S/L ratio from 0.07 to 0.10 g·mL^{-1} increased Ti recovery. From the acid concentration trend shown in Fig. 8(d), it is clear that the range of 10vol%–15vol% could be selected as the most ideal range of acidity. According to the milling energy diagram (Fig. 8(e)), intensifying the activation energy level from low to medium caused a significant improvement in Ti recovery. Afterwards, Ti recovery showed a slight decrease by increasing activation energy to the high level, which may be mainly due to agglomeration and lowered surface area. Hence, the medium energy level was considered to be the optimum energy level.

Leaching tests were performed at the optimum ranges designated by the Taguchi method. At this step, RSM was used to optimize effective parameters involved in the leaching process to achieve the highest Ti recovery (except for the milling energy and leaching time, where the optimum amounts of "medium level" and "3 h", respectively, were considered as constant parameters in RSM).

Using the experimental results, a quadratic response model was fitted to the data, considering the analysis of variance (ANOVA). This quadratic polynomial is as follows:

$$R_{\mathrm{T}} = 63.95 - 7.07B + 8.82C - 2.25AC + 2.50BC + 1.52A^2 \tag{6}$$

where R_{T} is Ti recovery. *A*, *B*, and *C* are temperature, S/L ratio, and HCl concentration, respectively. The correlation coefficient (R^2) for this model was calculated to be 0.82, which indicates that the model (Eq. (6)) fits adequately to the experimental data. As calculated by ANOVA, the effects of HCl concentration and S/L ratio as individual parameters and the interactions of temperature with HCl concentration (*AC*), S/L ratio with HCl concentration (*BC*), and individual parameter temperature are the largest. The model shows that variables *B* and *AC* have negative effects, and *C*, *BC*, and A^2 have a positive influence on Ti recovery.
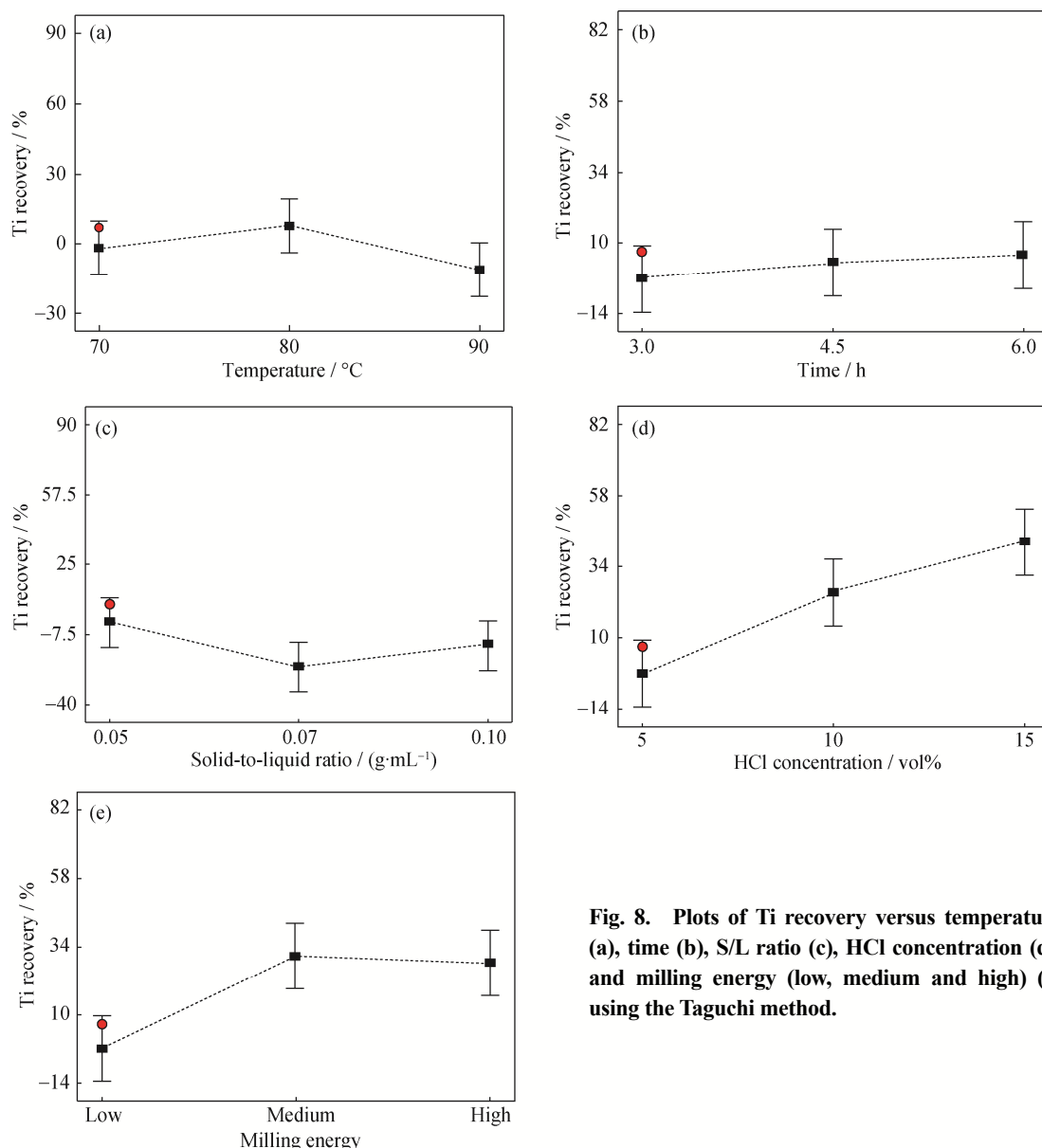
Fig. 8. Plots of Ti recovery versus temperature (a), time (b), S/L ratio (c), HCl concentration (d), and milling energy (low, medium and high) (e) using the Taguchi method.

The dependency of Ti recovery on acid concentration (*C*) and S/L ratio (*B*) and on acid concentration and temperature (*A*) are illustrated in 3D plots of interactions (*BC* and *AC*) in Fig. 9 where other influential parameters are fixed. Ti recovery enhances with simultaneous decrease of S/L ratio from 0.10 to 0.05 g·mL^{-1} and increase of HCl concentration from 10vol% to 15vol%, as shown in Fig. 9(a). The interaction of temperature and acid concentration shown in Fig. 9(b) reveals that the increase of temperature from 70 to 80°C leads to a higher Ti recovery. The effect of HCl concentration increment on Ti recovery is the same as that shown in Fig. 9(a). It can be concluded that an increase in temperature (*A*) and HCl concentration (*C*) and a decrease in S/L ratio (*B*) result in a higher Ti recovery.

According to Table 5, conditions applied for experiment number 5 were selected as the optimum leaching conditions resulting in the maximum Ti recovery of 80%. These conditions include leaching at 70°C within 3 h, S/L ratio of 0.05 g·mL^{-1}, HCl concentration of 15vol%, and medium mechanical activation of ilmenite concentrate (calculated as 25.38 kJ). Therefore, by applying the optimum energy level, the leaching process took place at a lower temperature, shorter time period, and lower acidity in comparison with the conditions reported by previous studies in which ilmenite was leached at 110°C, which is not an accessible temperature in ambient pressure and requires implantation of an autoclave [10]. Although leaching was performed using the same reducing agent as that used in previous re-

ports, it led to a high Ti leaching recovery at significantly reduced temperature and time. This was achieved through the addition of Fe in the milling stage. This enhancement was obtained mainly as a result of the following: (1) phase transformation, (2) powder refinement during milling

process, (3) minimization of atomic distances between Fe as a potential reducing agent and ilmenite as well as reducing the diffusion distance, and consequently (4) creation of structural defects leading to a partially amorphous structure.
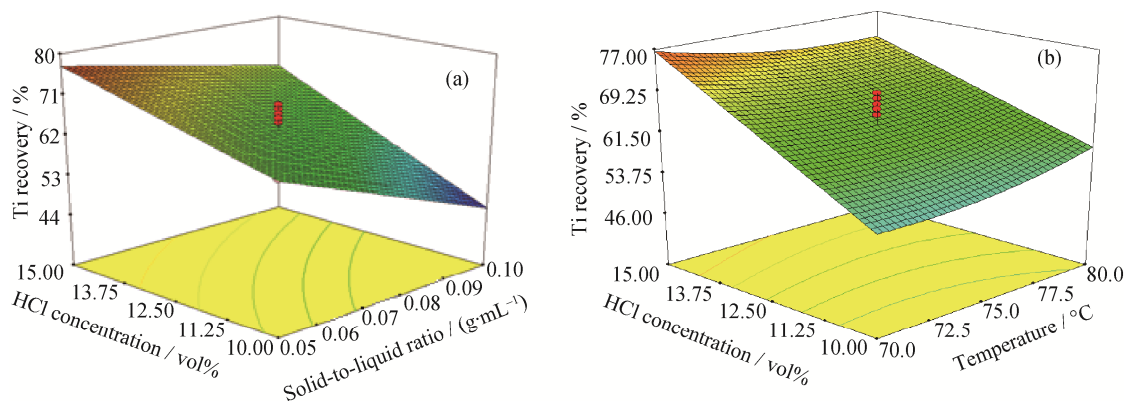

Fig. 9.   Three-dimensional plots for Ti recovery as a function of acid concentration and S/L ratio (a) and acid concentration and temperature (b).

4.3. Solvent extraction

To separate and purify Ti from Fe as the major impurity present in the leach liquor, solvent extraction was performed using TBP in kerosene as the extractant. Results of the solvent extraction process are summarized in Table 6. Titration results of the leach liquor showed that Fe was present in the chloride media in the form of Fe^{2+}, which is not extractable by TBP. Hence, solvent extraction with TBP is an efficient method for separation of Fe^{2+} from Ti.

The speciation of Ti, which mainly depends on the Eh, pH, and concentration of Ti in HCl solutions, directly affects its extraction behavior by various extractants. To determine Ti speciation in the optimized leaching condition (0.2 M Ti), an Eh–pH diagram was plotted using HSC 5.1 software, as shown in Fig. 10. At the Eh value and pH value of the solution in the optimized condition of 240 mV and 0.45, respectively, Ti mainly exists as $(TiO)^{2+}$ in the form of Ti(IV) in the solution.
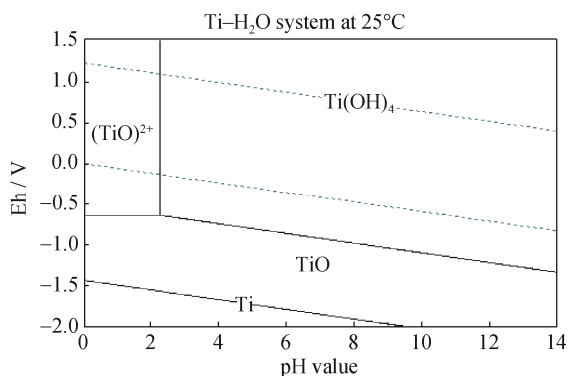

Fig. 10.   Eh–pH diagram of Ti in optimized leaching condition.

The extractant, TBP, is widely employed for Ti(IV) extraction via a solvating reaction. The Ti(IV) ions are extracted in the form of a neutral molecule associated with anions. Extraction of Ti(IV) by TBP is expressed as follows [25]:

$$TiOCl_2 + 2TBP = TiOCl_2TBP_2 \tag{7}$$

Neutral Ti(IV) molecules form by the following reaction [26]:

$$TiO^{2+} + 2Cl^- = TiOCl_2 , \beta = 3.55 \tag{8}$$
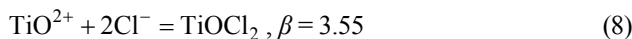
where β is the formation constant of $TiOCl_2$.

Incrementing the HCl concentration as well as the $CaCl_2$ in the solution increases the chloride concentration, which forces the above reaction to the right. Consequently, more neutral molecules of Ti are formed, which enhances extraction by the neutral organophosphorus reagents. The extraction of Ti from leach liquor was increased significantly by increasing the chloride ion concentration from the initial amount of 2.65 M to 10 M. Allal *et al.* [27] also showed that a considerable amount of Ti(IV) extraction by TBP normally occurs at chloride concentrations above 6 M and almost complete extraction is achieved at a chloride concentration of about 10 M. In this experiment, the effect of chloride concentration on the extraction efficiency was studied in the range of 2.65–10 M, while keeping the pH constant at 0.45. In the initial solution the chloride ions were generated from HCl that was introduced as the leaching agent in the leaching experiment. Thus, the concentration of the chloro-complexes in the initial aqueous solution was not sufficient for the extraction reaction to be performed. As shown in Table 6, no Ti was extracted from the initial solution. Gradual addition of $CaCl_2$ salt to the initial solution intro-

duced extra [Cl⁻] to the system and, consequently, extraction of Ti from the aqueous phase increased to 83%.

Table 6. Extraction of Ti(IV) from leach liquor by TBP in kerosene (initial Ti: 0.49 g/L)

$[Cl^-]^*$ / M	Ti extracted into organic phase / (g·L^{-1})	Ti in aqueous phase / (g·L^{-1})	Ti extracted / %
2.65	0.00	0.49	0
5.00	0.01	0.48	2
6.00	0.28	0.21	54
10.00	0.39	0.10	83

Note: * $CaCl_2$ + HCl.

5. Conclusions

(1) Intensifying the milling energy level from low to high resulted in crystallite size refinement of $FeTiO_3$ as well as elimination of silica and iron oxide reflections. The EDS maps revealed that the activation energy level increment from low to medium caused structural homogenization and refinement of the crystallite size ranging from 20 to 300 nm, consequently becoming suitable for rapid leaching.

(2) Mechanical activation in the three tested energy levels increased the leaching recovery of Ti from about 10% (in the absence of Fe) to 80%. Such enhancement was obtained mainly as a result of the combination of new surface area, an increase in internal and surface energy, and the formation of crystalline disorders in the mineral as well as the reduction in diffusion distance between Fe as a potential reducing agent and ilmenite. By applying the optimum energy level of 25.38 kJ, the leaching process took place at a lower temperature, shorter time period, and lower acidity than those reported in previous reports.

(3) The effective leaching parameters and optimum conditions were found to be: temperature range of 70–80°C, HCl concentration of 10vol%–15vol%, S/L ratio of 0.05 g·mL^{-1}, leaching time of 3 h, and medium mechanical activation energy of 25.38 kJ. Applying the optimum leaching conditions resulted in a Ti concentration in the leach liquor of 0.2 M.

(4) A model was proposed to calculate the Ti recovery as a function of temperature, S/L ratio, and HCl concentration.

(5) In the solvent extraction stage, an increase in the chloride ion concentration to 10 M had a significant impact on the extraction of Ti from the leach liquor by TBP, i.e., the extraction percentage increased from zero to 83%, increasing the separation of Fe (as the major impurity) from Ti.

References

[1] U. Diebold, The surface science of titanium dioxide, *Surf. Sci. Rep.*, 48(2003), No. 5-8, p. 53.

[2] T.S. Mackey, Acid leaching of ilmenite into synthetic rutile, *Ind. Eng. Chem. Prod. Res. Dev.*, 13(1974), No. 1, p. 9.

[3] T. Chernet, Applied mineralogical studies on Australian sand ilmenite concentrate with special reference to its behavior in the sulphate process, *Miner. Eng.*, 12(1999), No. 5, p. 485.

[4] C. Sasikumar, D.S. Rao, S. Srikanth, B. Ravikumar, N.K. Mukhopadhvay, and S.P. Mehrotra, Effect of mechanical activation on the kinetics of sulfuric acid leaching of beach sand ilmenite from Orissa, India, *Hydrometallurgy*, 75(2004), No. 1-4, p. 189.

[5] M. Jabłoński and A. Przepiera, Kinetic model for the reaction of ilmenite with sulphuric acid, *J. Therm. Anal. Calorim.*, 65(2001), No. 2, p. 583.

[6] E.A. Abdel-Aal, I.A. Ibrahim, A.A.I. Afifi, and A.K. Ismail, Production of synthetic rutile from Egyptian ilmenite ore by a direct hydrometallurgical process, [in] *2nd International Conference on Processing Materials for Properties*, San Francisco, 2000, p. 955.

[7] C. Li, B. Liang, H. Song, J.Q. Xu, and X.Q. Wang, Preparation of porous rutile titania from ilmenite by mechanical activation and subsequent sulfuric acid leaching, *Microporous Mesoporous Mater.*, 115(2008), No. 3, p. 293.

[8] K.K. Sahu, T.C. Alex, D. Mishra, and A. Agrawal, An overview on the production of pigment grade titania from titania-rich slag, *Waste Manage. Res.*, 24(2006), No. 1, p. 74.

[9] M.H.H. Mahmoud, A.A.I. Afifi, and I.A. Ibrahim, Reductive leaching of ilmenite ore in hydrochloric acid for preparation of synthetic rutile, *Hydrometallurgy*, 73(2004), No. 1-2, p. 99.

[10] B.N. Akhgar, M. Pazouki, B.N. Akhgar, M. Ranjbar, and A. Hosseinnia, Preparation of micro and nanostructured titania compounds from ilmenite concentrate, *Int. J. Miner. Process.* 124(2013), p. 138.

[11] J.Y. Xiang, S.L. Liu, X.W. Lv, and C.G. Bai, Preparation of rutile from ilmenite concentrate through pressure leaching with hydrochloric acid, *Metall. Mater. Trans. B*, 48(2017), No. 2, p. 1333.

[12] N.Y. Mostafa, M.H.H. Mahmoud, and Z.K. Heiba, Hydrolysis of $TiOCl_2$ leached and purified from low-grade ilmenite mineral, *Hydrometallurgy*, 139(2013), p. 88.

[13] E.J. Kelley, *Modern Aspects of Electrochemistry*, J.O'M. Bockris, B.E. Conway, and R.E. White, eds., Springer, Boston, 1982, p. 319.

[14] F.A. Cotton and G. Wilkinson, *Advanced Inorganic Chemistry: A Comprehensive Text*, 4th Ed., John Wiley & Sons Inc., New York, 1980, p. 692.

[15] K.C. Sole, Recovery of titanium from the leach liquors of titaniferous magnetites by solvent extraction: Part 1. Review of the literature and aqueous thermodynamics, *Hydrometallurgy*, 51(1999), No. 2, p. 239.

[16] I. Cservenyák, G.H. Kelsall, and W. Wang, Reduction of Ti^{IV} species in aqueous sulfuric and hydrochloric acid I: Titanium

speciation, *Electrochim. Acta*, 41(1996), No. 4, p. 563.

[17] C. Suryanarayana, Mechanical alloying and milling, *Prog. Mater. Sci.*, 46(2001), No. 1-2, p. 1.

[18] N. Burgio, A. Iasonna, M. Magini, S. Martelli, and F. Padella, Mechanical alloying of the Fe–Zr system, Correlation between input energy and end products, *IL Nuovo Cimento D*, 13(1991), No. 4, p. 459.

[19] M. Magini, A. Iasonna, and F. Padella, Ball milling: an experimental support to the energy transfer evaluated by the collision model, *Scripta Mater.*, 34(1996), No. 1, p. 13.

[20] B.S. Murty, M. Mohan Rao, and S. Ranganathan, Milling maps and amorphization during mechanical alloying, *Acta Metal. Mater.*, 43(1995), No. 6, p. 2443.

[21] S. Kehoe, M. Ardhaoui, and J. Stokes, Design of experiments study of hydroxyapatite synthesis for orthopaedic application using fractional factorial design, *J. Mater. Eng. Perform.*, 20(2011), No. 8, p. 1423.

[22] M. Ghadiri, A. Vatanara, D. Doroud, and A.R. Najafabadi, Paromomycin loaded solid lipid nanoparticles: Characterization of production parameters, *Biotechnol. Bioprocess Eng.*, 16(2011), No. 3, p. 617.

[23] G.M. Venkatesh, J.A.N. Coleman, T.J. Wrzosek, S. Duddu, N.R. Palepu, R. Bandyopadhyay, and D.J.W. Grant, Fractional factorial designs for optimizing experimental conditions for Hiestand's Indices of Tableting Performance, *Powder Technol.*, 97(1998), No. 2, p. 151.

[24] G.H. Jeffery, J. Bassett, J. Mendham, and R.C. Denney, *Vogel's Textbook of Quantitative Chemical Analysis*, 5th Ed., John Wiley & Sons Inc., New York, 1989, p. 376.

[25] E. Narita, H. Takeuchi, H. Ichikawa, T. Odagawa, and T. Okabe, Manufacture of pure titanium(IV) oxide by the chloride process: II. Selective extraction of titanium (IV) and iron(III) from hydrochloric acid leach liquor of ilmenite ore by tributyl phosphate, *Bull. Chem. Soc. Jpn.*, 56(1983), No. 6, p. 1832.

[26] S. Kotrly and L. Sucha, *Handbook of Chemical Equilibria in Analytical Chemistry*, Ellis Horwood Ltd., Chichester, 1985, p. 414.

[27] K.M. Allal, D. Hauchard, M. Stambouli, D. Pareau, and G. Durand, Solvent extraction of titanium by tributyl phosphate, trioctylphosphine oxide and decanol from chloride media, *Hydrometallurgy*, 45(1997), No. 1-2, p. 113.